GEOFIZIKA VOL. 38 2021

DOI: https://doi.org/10.15233/gfz.2021.38.10
Original scientific paper

Geodetic and seismological analysis of the CROPOS ZAGR station kinematics during the Zagreb 2020 M_L 5.5 earthquake

Danijel Šugar [1], Željko Bačić [1] and Iva Dasović [2]

[1] Faculty of Geodesy, University of Zagreb, Zagreb, Croatia

[2] Department of Geophysics, Faculty of Science, University of Zagreb, Zagreb, Croatia

Received 7 July 2021, in final form 23 December 2021

The CROPOS's ZAGR stations, one of 33 stations of the Croatian permanent GNSS (Global Navigation Satellite System) network CROPOS (Croatian Positioning System), is located in Zagreb's city centre. For the first time, motion of one of the CROPOS stations (the ZAGR station) during an earthquake shake (the Zagreb 2020 M_L5.5) was analysed by the PPK (Post-Processed Kinematic) method using all available GNSS signals (GPS – Global Positioning System, GLONASS – *GLObalnaya NAvigatsionnaya Sputnikovaya Sistem*, Galileo, BeiDou) and seismologically interpreted. The ZAGR station is situated about 9 km to the south-southeast of the earthquake's epicentre. The analysis showed that the station's movements, *i.e.* combined surface and building motion, during the shake was far above the noise level and enabled the assessment of the station's kinematics: movements in the range of approx. 13 cm in direction north–south (N–S) and approx. 6 cm in direction east–west (E–W). However, movements in the vertical direction were slightly above the noise level. Even though the ZAGR station kinematic behaviour was pronounced, no permanent displacement was identified. The seismological analysis showed that the ZAGR station recorded the onset of the SV-waves on the N–S component, surface waves on the N–S (predominantly Rayleigh waves) and E–W (mainly Love waves) components. The resolution of 1 s of the results of the PPK method have enabled a thorough analysis of the ZAGR station kinematics and pointed out the usefulness of the method in earthquake observations.

Keywords: CROPOS, earthquake, GNSS, kinematic motion, PPK

1. Introduction

1.1. Seismicity of the continental part of Croatia and the Zagreb 2020 M_L 5.5 earthquake

Continental part of Croatia is characterized by low to moderate seismicity and rare occurrence of strong earthquakes: its north-western part is one of the

seismically most active areas, especially in the Medvednica Mt. and Zagreb area (Ivančić et al., 2018). One of the most significant earthquakes in the Zagreb epicentral area is certainly the Great Zagreb Earthquake that occurred on 9th November 1880: the maximum intensity was estimated as VIII MSK (Medvedev-Sponheuer-Kárnik macroseismic scale) and the epicentre in Medvednica Mt. near Čučerje, NE (north-east) from the Zagreb city centre, with the macroseismic magnitude estimated as 6.1 (after Herak et al., 2021 and Latečki et al., 2021). After that, the events of significant magnitude happened in 1901, 1905, 1906, and 1990: the 1990 earthquake had $M_L = 5.0$ with epicentre to the NW (north-west) of the Zagreb (Dasović et al., 2020; Šavor Novak et al., 2020; and references within) and was the last moderately strong earthquake in the Medvednica Mt. epicentral area. Historical records, seismological and seismotectonic investigation suggest that the earthquake of up to approx. $M = 6.5$ can be expected for the area (Tomljenović, 2020; Markušić et al., 2020; Dasović et al., 2020; Šavor Novak et al., 2020). Analysis of the earthquake catalogue presented in Ivančić et al. (2018) indicates that the continental part of Croatia is capable for one $M_W = 5.0$ event per year or one $M_W = 6.4$ earthquake per century. The Seismic Hazard Map for the Republic of Croatia (Herak et al., 2011) shows maximum ground accelerations for Zagreb approx. 0.25 g, which is one of the highest hazards in the country.

On 22nd March 2020 05:24 UTC, the wider area of the City of Zagreb was struck by a moderately strong earthquake of local magnitude $M_L = 5.5$ (moment magnitude $M_W = 5.3$ or 5.4, depending on the source) with the epicentre in Markuševec, approx. 9 km to the NE from the centre of the city, and at approx. 8 km of depth (Šavor Novak et al., 2020; Seismological Survey of the Department of Geophysics, Faculty of Science, University of Zagreb, Tab. 2). Soon after followed the strongest aftershock at 06:01 UTC with $M_L = 4.9$ ($M_W = 4.7$). The macroseismic intensity at the epicentre and in the historical city centre was estimated as VII EMS (European macroseismic scale; Seismological Survey, 2020) and one human life was lost. The reported earthquake source mechanisms obtained with different methods and from different authors are in very good agreement and suggest a predominantly reverse fault oriented toward ENE with a dip of 47° (Herak et al., 2021). The spatial distribution of the aftershock hypocentres supports those findings (Herak et al., 2021, Šavor Novak et al., 2020) as well as very preliminary results obtained by the InSAR method (Govorčin, 2020). Šavor Novak et al. (2020) reported that more than 1400 aftershocks occurred in the first 45 days of the series, with 10 events having $M_L \geq 3.0$ and 724 earthquakes with $M_L > 1.0$. The peak ground acceleration reported for two locations in Zagreb was 0.22 g and 0.20 g (Šavor Novak et al., 2020 and references within). Considerable damage was reported for the buildings in the epicentral area, but the most notable damage was documented on the old and poorly maintained buildings in Zagreb's historical city centre. In many cases, those building heav-

ily impacted by the earthquake are part of the cultural heritage, the most prominent member being the Cathedral of Zagreb.

1.2. Galileo and other global navigation satellite systems

At present, the term GNSS includes four globally available navigation satellite systems: the American GPS (Global Positioning System), the Russian GLONASS (rus. GLObalnaya NAvigatsionnaya Sputnikovaya Sistema), the Chinese BeiDou, and the European Galileo. Common features of all those systems are the satellites in MEO (Medium Earth Orbit) orbits, broadcasting multifrequency signals in L-band (1–2 GHz) with global availability. More information about the individual systems can be found on the following websites: https://www.gps.gov/ (GPS), https://www.glonass-iac.ru/en/ (GLONASS), http://en.beidou.gov.cn/ (BeiDou) and https://www.gsc-europa.eu (Galileo). Additionally, plenty of useful information about GNSS can be found in the European GNSS Agency (2020). Currently (December 2021), the Galileo constellation encompasses 28 satellites, one of them being unavailable, additional three satellites being 'not usable', 2 satellites are 'under commissioning' and the remaining 22 satellites are set to be usable (https://www.gsc-europa.eu/system-service-status/constellation-information). Once fully operational, the Galileo system will provide five high-performance services worldwide: Open Service (OS), Public Regulated Service (PRS), High Accuracy Service (HAS), Commercial Authentication Service (CAS) and Search and Rescue Service (SAR). Galileo officially progressed from a testing phase to the provision of live services in 2016 with the declaration of Galileo Initial Services. Galileo navigation signals are transmitted in four frequency bands (E5a, E5b, E6, and E1) which provide a wide bandwidth for Galileo signals transmission. Benedicto and Da Costa (2020) outlined future development plans of the Galileo system including the production of 12 additional Batch 3 Galileo first-generation satellites which will be ready for launch from middle 2021 onward. Currently, the system is being built toward the Full Operational Capability: the first two Galileo satellites of Batch 3 (27 and 28) were launched by Soyuz launcher from Europe's Spaceport in French Guiana on 5th December 2021 (European Space Agency, 2021b). The Galileo Second Generation (G2) satellites will be much larger; they will use electric propulsion for the first time and host an improved navigation antenna. Their fully digital payloads are being designed to be easily reconfigured in orbit, to enable them to actively respond to the evolving needs of users with new signals and services (European Space Agency, 2021a). The first launch of G2 satellites is scheduled to take place by the end of 2024 (Maufroid et al., 2021).

1.3. The CROPOS network

The CROatian POsitioning System (CROPOS) network is a network of 30 permanent GNSS stations uniformly spread across Croatian territory estab-

lished in 2008 by the State Geodetic Administration (SGA) of the Republic of Croatia. The network was broadened with three additional stations on Croatian territory, and overall 18 stations from neighbouring countries (Slovenia 7, Hungary 4, Bosnia and Herzegovina 5, and Montenegro 2). At present, the networked solution includes data from 51 stations (Fig. 1).

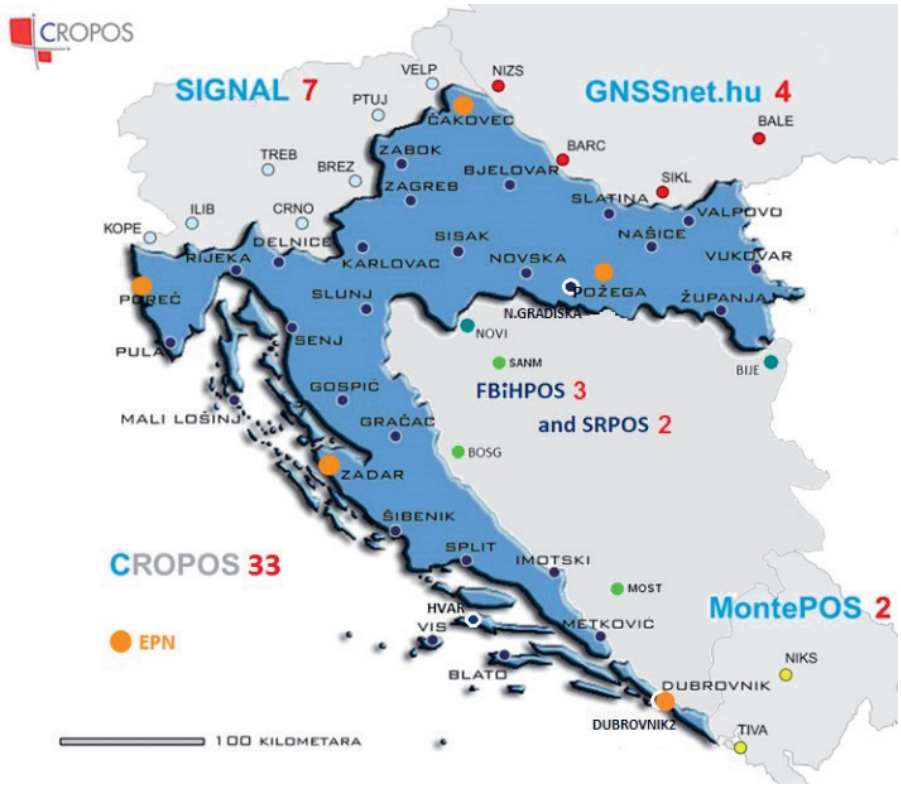

Figure 1. CROPOS network (https://www.cropos.hr/).

Since its establishment, the control centre of CROPOS has been updated in terms of software and hardware. In 2019, the network was upgraded by the installation of the newest GNSS receiver Trimble Alloy and accompanying GNSS antenna Zephyr Geodetic 3 w/TZGD at each station (https://geomatika-smolcak.hr/novosti/modernizacija-cropos-sustava/). The software platform of the control centre was updated to Trimble Pivot Platform (TPP) ver. 4.1.3. All installed GNSS receivers and antennas are multi-frequency and multi-constellation receivers capable of receiving signals of GPS, GLONASS, Galileo, and BeiDou satellites. Galileo signals recorded by the GNSS receivers Trimble Alloy installed at each CROPOS station were in frequency bands E1, E5a, E5b, and E5 AltBOC

(Open Service). CROPOS offers three services, two of which are widely used by the surveying community in Croatia: VPPS (Networked Real-Time Kinematic) and GPPS (observations used for Post-processing applications). Magaš (2021) investigated the impact of the modernization of CROPOS on the performance of services and he concluded that the modernization did not ensure a substantial enhancement in terms of accuracy, but it did improve the reliability and availability. Additionally, Kliman (2021) showed that Galileo as a system is capable of providing reliable individual solutions within the modernized CROPOS network even if it has not already reached its Full Operational Capability.

1.4. Overview of the GNSS methods for the earthquake effects assessment

In the last twenty years, several studies reported kinematic analysis of GNSS stations during the earthquake shaking, mostly caused by a (very) strong earthquake ($M_W \geq 6$) when close enough to the events hypocentre (*e.g.* Larson et al., 2003; Grapenthin and Freymueller, 2011; Xu et al., 2013; Hohensinn and Geiger, 2018). They most often use the Precise Point Positioning (PPP) method. These studies show that the high-rate GNSS measurements usually record displacement of S-waves and surface waves. Paziewski et al. (2020) showed that is even possible to record changes in displacement wavefield generated by the weak to moderate earthquake ($M_W = 3.8$) near the station. For the GNSS stations in Croatia, Ganas et al. (2021) shortly presented the recordings of the motion at the BJEL station (CROPOS) caused by Petrinja $M_W = 6.4$ mainshock.

Zumberge et al. (1997) introduced the PPP method as an alternative to differential GNSS positioning in the late 1990s. The PPP approach uses undifferenced, dual-frequency, pseudorange and carrier-phase observations together with precise satellite orbit and clock products, for standalone static or kinematic geodetic point positioning with centimetre precision (Kouba et al., 2017; Glaner and Weber, 2021). Unlike the traditional double-differenced (DD) relative baseline positioning, PPP does not demand simultaneous observations at two stations. However, this requires the introduction of additional initial phase ambiguity unknowns, causing a relatively long (up to 15 min or longer) initial convergence of PPP solutions. The elimination of errors by differencing in relative positioning techniques is replaced by precisely modelling many of the error sources in PPP (Weston and Schwieger, 2014). A comprehensive overview of the correction biases or errors to be modelled or otherwise accounted for in the case of PPP compared to differential positioning techniques is given in Rizos et al. (2012). A relatively long convergence time, *i.e.* the duration of continuous observations needed to achieve a certain accuracy level, is a limitation of the PPP method. The convergence time in the PPP method can be shortened dramatically with an increasing number of continuously observed satellites (Lipatnikov and Shevchuk, 2019). The reduction in the convergence time is a major topic in scientific research, and to make the PPP method more competitive among other high-precision GNSS positioning techniques, researchers have tested different

approaches (Glaner and Weber, 2021). The increased popularity of the PPP method for geodetic (*e.g.* determination of the coordinates of receivers for the densification of the ITRF datum) and many other applications, for example in earthquake studies (*e.g.* determination of pre-, co- and post-seismic motion), meteorology (*e.g.* estimation of tropospheric delay) etc. was spurred by the availability of precise orbit and clock solution products in the late 1990s (Rizos et al., 2012).

Our study presents, for the first time, an analysis of the earthquake caused motion in Croatia by the kinematic GNSS method leveraging the signals of all Global Navigation Satellite Systems. This is a detailed study of the GNSS processing results of the ZAGR station measurements obtained by the PPK method in order to analyse the kinematic motion of the station during the shake and determine whether a permanent displacement at the station site was caused by the Zagreb 22nd March 2020 M_L = 5.5 earthquake and its shaking. The first preliminary results of the PPK processing were presented in Šugar and Bačić (2021). The PPP method is recently a preferred GNSS method for assessing seismic displacements and this can be explained by the main disadvantage of relative positioning (RP): the solutions are influenced by movements of the reference stations (Li et al., 2013). Therefore, in our study we have applied the relative positioning technique PPK guided by the following: (i) the reference station (ZABO) hasn't been significantly influenced by co-seismic motion, (ii) the distance between stations is pretty short enabling a reliable ambiguity resolution and (iii) preliminary PPP solution has shown to be burdened with a substantial amount of noise and bias.

2. Data and methods

2.1. The CROPOS ZAGR and ZABO stations data

Three technical faculties of the University of Zagreb, namely the Faculty of Geodesy (GEOF), the Faculty of Civil Engineering (GRAD) and the Faculty of Architecture (AF), are headquartered in the same building (also known as the AGG building), less than 2 km from Zagreb's central square. One of the stations of the CROPOS network is located atop that building. Although the average distance between CROPOS stations across the national territory is 70 km, the closest station to the ZAGR station is located in Zabok (ZABO), at a distance of approx. 25 km (see Fig. 1). Within the project of CROPOS modernization, the newest GNSS receivers Trimble Alloy with the associated GNSS antennas Trimble Zephyr 3 Geodetic w/TZDG were installed at both stations. Figures 2 and 3 show the GNSS antennas at the CROPOS stations ZAGR and ZABO, respectively. Observation data collected at both stations were downloaded from the CROPOS GPPS available at http://195.29.198.194/Map/SensorMap.aspx.

Figure 2. The GNSS antenna of the CROPOS ZAGR station.

Figure 3. The GNSS antenna of the CROPOS ZABO station.

The earthquake mainshock occurred on 22nd March 2020 at 05:24 UTC. Data recorded with logging interval of 15 s were downloaded for both stations for the whole day of 22nd March 2020 (time window of 24 h that begins at 00:00:00 GPST and ends at 23:59:59 GPST). These data were used to check for the accuracy of the ZAGR station coordinates, even though the coordinates of all CROPOS stations were precisely determined in ETRF2000 (R05), epoch = 2008.83. Observation data with logging interval of 1 s for the hour of the mainshock, *i.e.* time window 5–6 GPST, were downloaded from CROPOS GPPS for both stations. These observation data were used for the PPK processing and determination of a kinematic solution for the ZAGR station.

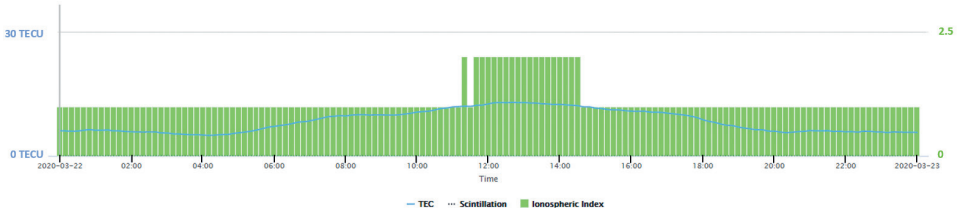

Figure 4. Information on ionospheric condition for 22nd March 2020 (0–24 UTC): total electron content *(TEC)*, scintillation and the ionospheric index according to https://www.gnssplanning.com/#/charts.

To provide the environment for a reliable solution determination, a time window for the whole day 22nd March 2020 (0–24 UTC) was examined for ionospheric conditions using GNSS online Planning Tool (https://www.gnssplanning.com/#/charts). As shown in Fig. 4, the ionospheric index, total electron content (*TEC*), and scintillation were at their minimum, consequently contributing to a reliable solution determination.

Local conditions related to a reliable observation acquisition at both stations, the ZAGR and ZABO stations, were assessed by the TEQC software (https://www.unavco.org/software/data-processing/teqc/teqc.html). Processing in TEQC was carried out using observation and broadcast ephemeris files enabling a full quality check (qc-full). As a part of the QC Summary Report, the most interesting reported quantities are the RMS (root mean square) moving average of the multipath combinations (*MP12*, *MP21*, *MP15*, *MP51*) as well as the mean of the signal-to-noise (SNR) ratio for L1, L2, and L5 signals (*S1*, *S2*, *S5*). Multipath combinations refer to linear combinations of the pseudorange and carrier phase observations between different carriers (Estey and Wier, 2014). Along with the mean *S* values (*S1*, *S2*, *S5*), the standard deviation (*sd*) values and the number of values (*n*) used to compute them are given. The summary of TEQC computing for stations ZAGR and ZABO is given in Tab. 1.

The comparison of multipath moving average (*MP*) and SNR means (*S*) values computed for the stations ZAGR and ZABO shows that multipath conditions are slightly better for the ZAGR station, whereas the SNR conditions are slightly better for the ZABO station. Nevertheless, the observation environment at both stations can be regarded as favourable enabling high-quality GNSS data and leading to a reliable coordinate computation. The estimation of site (station) suitability for GNSS measurement has been carried out according to the procedure outlined in Šugar et al. (2016).

Table 1. Values of multipath RMS moving-average (MP), signal-to-noise ratio mean (S) with standard deviation (sd) and the number of values (n) used to compute them according to TEQC for stations ZAGR and ZABO for 22nd March 2020, 5–6 GPST.

		Stations	
		ZAGR	ZABO
RMS moving average of the multipath combinations	*MP12* [m]	0.233238	0.250414
	MP21 [m]	0.222895	0.277490
	MP15 [m]	0.289833	0.291149
	MP51 [m]	0.156421	0.169964
Mean of the signal SNR	*S1 (sd,n)*	45.76 (4.65, 87420)	45.51 (4.66, 88850)
	S2 (sd,n)	39.71 (7.58, 49076)	39.63 (7.53, 49102)
	S5 (sd,n)	45.30 (5.06, 45511)	45.12 (5.03, 46885)

2.2. Relative static and kinematic processing of ZAGR and ZABO stations data

Although the station coordinates of the CROPOS network are accurately determined and known in ETRF2000 (R05) (e = 2008.83), static vector between stations ZABO and ZAGR was processed: the ZABO station coordinates were held fixed, and subsequently, coordinates of the ZAGR station were obtained. The obtained solution was regarded as a reference for the subsequent analysis. Such an approach was embraced because several parameters may influence a relevant coordinates comparison (*e.g.* epoch of observation, ephemerides, satellite systems used, different baseline processing engines and SWs used, number of stations involved, etc.). In this study, all the coordinates presented were computed in the official geodetic reference system HTRS96/TM (Croatian Terrestrial Reference System 1996 / Transverse Mercator) for Easting (E) and Northing (N) plane coordinates and official vertical referent system HVRS71 (Croatian Height Reference System for the epoch 1971.5) for height H. Static baseline processing was carried out in the professional software package Trimble Business Center (TBC; ver. 5.3) using observations with logging interval 15 s of all available GNSS signals (GPS, GLONASS, Galileo, and BeiDou), elevation mask 10°, and broadcast ephemerides. TBC is a program package with a GPS processing engine introduced in 2005. Over time, a GNSS engine has evolved, and since the ver. 3.5 (released in 2015), it supports the independent GNSS constellation solutions including BeiDou-only, GLONASS-only, and BeiDou + GLONASS-only combinations. Starting with the TBC, ver. 3.90, Galileo-only post-processing baseline solution was enabled as well (Šugar et al., 2018). In version 4.0 (released in 2017), a modernized approach for static GNSS baseline processing was introduced – multiple processing modes dynamically chosen according to the baseline length and duration of observation sessions (Blecha, 2018).

In order to compute the ZAGR station coordinates and estimate baseline components precision, the coordinates of the ZABO station were held fixed during the baseline processing. The estimate of the baseline components precision can be considered as an assessment of the ZAGR coordinates precision, given with 95% level of confidence: ± 0.002 m (E), ± 0.002 m (N), ± 0.010 m (H). When compared, coordinates of the ZAGR station calculated by the static single baseline ZABO-ZAGR solution (24-hour time window) and the official coordinates, gave the differences of –0.005 m for Easting, –0.008 m for Northing, and 0.013 m in height. This result proved that the obtained daily static solution may be regarded as reliable and that allowed the subsequent analysis. If taken into consideration the declared accuracy of the CROPOS GPPS (< 1 cm), the accuracy of the static method itself and the fact that the official coordinates were determined with different software, different reference stations, different ephemeris data, and different time window, the coordinates calculated by a single-baseline solution can be considered as highly reliable therefore yielding a robust base for further kinematic solutions analysis.

2.3. The Post-Processed Kinematic (PPK) method

The Post-Processed Kinematic (PPK) method belongs to a relative positioning method involving at least two GNSS receivers observing simultaneously the same satellites. The method is primarily used for coordinates determination, and the phase ambiguities have to be resolved leading to the ambiguity fixed solution. In order to resolve the ambiguities kinematically, dual-frequency receivers require up to 1–2 min of observations for baselines lengths of up to 20 km. Estimates can be done for a 10 km long baseline and dual-frequency observations at dozen epochs, which will result in a position accuracy of 2 cm (Hofmann-Wellenhof et al., 2008). Šugar et al. (2016), Bačić et al. (2017) and Blaženka et al. (2018) showed the potential of the PPK method to obtain results with 1–2 cm level of accuracy even for much smaller baselines length. However, that accuracy level has been mainly achieved for substantially longer baselines (*e.g.* 25 km), as will be shown and discussed later.

We used the PPK method to compute kinematic solution for the ZAGR station on time series of coordinates recorded with interval 1 s (1 Hz logging rate). In this case, the PPK processing involved the baseline between the stations ZABO and ZAGR with a length of more than 25 km. Before the data processing, we estimated that a reliable solution at such a distance (baseline length) would be feasible. Indeed, this is the first time that this method was used in processing GNSS (GPS, GLONASS, Galileo, and BeiDou) data enabling the kinematic and seismological analysis of earthquake effect on a permanent GNSS station of the CROPOS network.

After the static baseline between the ZABO and ZAGR stations was processed and the coordinates of the ZAGR station were estimated along with their precision, the PPK computations were launched. An hour-long (5–6 GPST) time series, with a 1 Hz sampling rate, recorded at the stations ZABO and ZAGR were kinematically processed, providing coordinates of the ZAGR station for each second. Out of possible 3600 epochs in the time window 5–6 h GPST, 3599 PPK solutions of the ZAGR station with fixed ambiguities were computed enabling further analysis. GPS observations are referenced to the GPS Time (GPST) but calculated signals are displayed in UTC (Universal Time Coordinated) because the seismological data are given in this time system. The difference between these two time systems is: GPST – UTC = 18 s.

After the PPK processing, the statistics of Easting (E), Northing (N), and Height (H) values were analysed. Furthermore, distances in the horizontal plane between each one-second $PPK(i)$ solution and daily (24 h) static solution $STATIC$, from their Eating and Northing, were calculated as

$$dist[PPK(i) - STATIC] = + \sqrt{\{E[PPK(i)] - E(STATIC)\}^2 + \{N[PPK(i)] - N(STATIC)\}^2} \,. \quad (1)$$

2.4. Seismological data

The mainshock information (time of origin, epicentre coordinates, hypocentre depth and magnitude; Tab. 2) were provided by the Croatian Seismological Survey, Department of Geophysics, Faculty of Science, University of Zagreb (CSS) and data were taken from EMSC (European-Mediterranean Seismological Centre, 2020) and USGS (United States Geological Survey, 2020).

Distance between two epicentres derived by CSS and EMSC is 1.6 km, which is within the 95 % ellipse of confidence (semimajor axis 2.9 km reported by

Table 2. Time of origin, epicentre coordinates, hypocentre depth and magnitude of the mainshock reported by CSS, EMSC and USGS.

Source	CSS	EMSC	USGS
Time of origin	05:24:03.1 UTC	05:24:02.8 UTC	05:24:03.7 UTC
Latitude	45.884°	45.87°	45.907°
Longitude	16.013°	16.02°	15.970°
Depth	8.3 km	10 km	10 km
Magnitude	$M_L = 5.5$	$M_W = 5.4$	$M_W = 5.3$

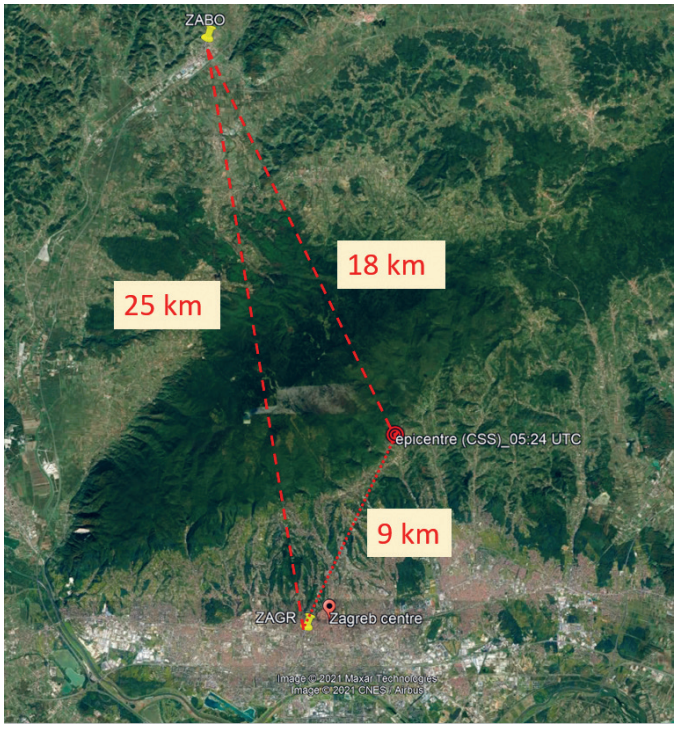

Figure 5. Distances between the estimated earthquake epicentre and the CROPOS stations ZAGR and ZABO (Google Earth).

EMSC). The time difference between origins is 0.3 s, which is below the RMS travel time residual of 0.93 s reported by EMSC. Epicentre location estimated by USGS is approx. 5 km far apart from the two, therefore it will not be taken into further consideration. Parameters determined by the CSS were taken as the reference ones and as such they were used in the analysis of the earthquake effects. The distance between the epicentre (CSS) and the stations ZAGR and ZABO is 9.3 km and 18.1 km, respectively, whereas the distance between CROPOS stations ZAGR and ZABO is 25.0 km (Fig. 5).

3. Results and discussions

The ZAGR station is located only about 9 km from the mainshock epicentre in the Zagreb city centre where earthquake shaking was very strong, and many old and historical heritage buildings experienced considerable damage. Therefore, we assumed that the shake itself could be registered, assessed and analysed by a kinematic solution. As previously stated, the PPK method is a relative method, therefore observations from at least two GNSS stations are necessary to obtain a solution. The nearest to the ZAGR station, and having the potential of providing a reliable solution, is the ZABO station that is approx. 25 km to the north of the ZAGR station and about 18 km away from the mainshock epicentre (Fig 5).

3.1. Results of the PPK method for the ZAGR station

The analysis of the results of the PPK processing of the 1-hour-long time window (5–6 GPST) has shown large values, particularly in ranges between maximum and minimum values (Range = Max – Min): $\Delta E = 0.059$ m, $\Delta N = 0.132$ m and $\Delta H = 0.047$ m – this was far above the expected level of noise, especially for Easting and Northing components.

Because the largest range was found in Easting and Northing components, distances between each 1-s *PPK*(*i*) solution and static daily solution *STATIC* were calculated (see Eq. 1) and plotted against time, as shown in Fig. 6. Values of *dist* [*PPK*(*i*) – *STATIC*] are mostly below 20 mm (max. 25 mm); therefore, we can consider this value as a noise level normally present in the PPK solutions. However, a prominent spike with the peak value of 8.6 cm at 05:24:11 UTC is seen several seconds after the origin time of the earthquake (Tab. 2), but no noticeable and significant permanent displacement has been obtained. In particular, distances between the individual *PPK*(*i*) solutions before and after the earthquake (05:24 UTC) remained chiefly unchanged.

Figure 7 shows the height H of the ZAGR station computed for each epoch compared to daily (24 h) static solution *STATIC*. The height H shows a noise within ± 24 mm around the daily static solution, which is approximately equal to a half of the ΔH value. Although the vertical accuracy is normally 1.5–2 times worse than the horizontal one (Hofmann-Wellenhof et al., 2008), it seems that in this case, they are approximately equal. Unlike horizontal components, H values

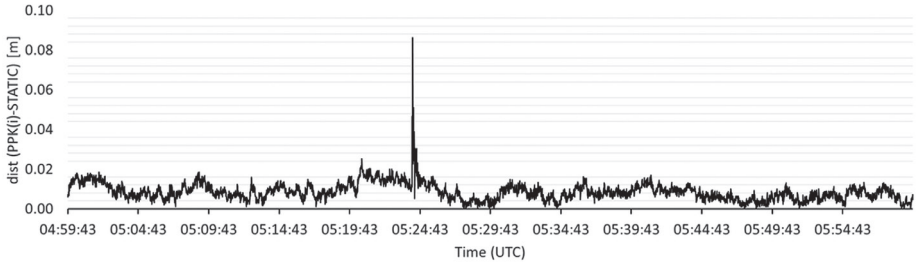

Figure 6. Distance between each *PPK*(*i*) solution for the time window 5–6 GPST (22nd March 2020) and the reference daily static (24 h) solution *STATIC* (22nd March 2020), shown in UTC.

do not display any prominent spike around the time of the earthquake at 05:24 UTC. Similar to horizontal components, height also shows no significant and noticeable permanent displacement. Therefore, we can conclude that the mainshock has not caused any significant permanent displacement.

The CSS reported the occurrence of four aftershocks with $M_L \geq 2.5$ in the analysed time window of 5–6 UTC (05:26:23.3 UTC $M_L = 2.7$, 05:28:34.9 UTC $M_L = 2.9$, and 05:29:35.4 UTC $M_L = 3.3$). However only mainshock is well visible in Fig. 6 as a spike and these aftershocks are not visible in Fig. 6 nor Fig. 7 – this is to be expected because these are considerably weaker earthquakes.

It should be noted that recent scientific research activities (a dedicated scientific paper on that topic is being prepared) have shown that the ZABO station was slightly influenced by the Zagreb 2020 M_L 5.5 earthquake. This is consistent with data provided by USGS (United States Geological Survey) related to the ground shaking (*e.g.*, *PGA* – peak ground acceleration) caused by the earthquake (United States Geological Survey, 2020). However, this does not compromise the achievement of a reliable PPK solution for the ZAGR station.

The results obtained in this analysis, especially in Easting and Northing showing a prominent change in distance in a horizontal plane relative to the reference daily static solution, deserve a more detailed analysis.

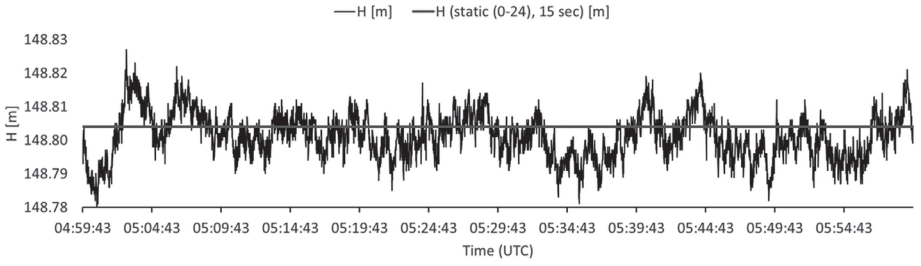

Figure 7. Height of the ZAGR station computed by the PPK method (black thin line) for each epoch for the time window 5–6 GPST on 22nd March 2020 compared to the reference daily static (24 h) solution for 22nd March 2020 (grey thick horizontal line), shown in UTC.

3.2. Analysis of the PPK results around the time of the earthquake

A subset of the PPK results around 05:24 UTC was selected and subjected to further analysis. Considering the origin time of the mainshock (Tab.e 2) and some time needed for seismic waves to reach the ZAGR station, we inspected the 88-s-long time window of relative displacement in horizontal plane *dist*[*PPK*(*i*) – *STATIC*] that begins 30 s before the seismic wave's onset at the ZAGR station and ends 30 s after it attenuates into the noise level (Fig. 8). The numerical analysis of the obtained signal and visual inspection of the figure, have led to the conclusion that the earthquake shaking affected with certainty the ZAGR station motion for 29 s, with the beginning at 05:24:09 UTC and the end at 05:24:38 UTC. The largest departure from the daily static solution of 8.6 cm was registered at 05:24:11 UTC; thereafter the oscillations attenuate until they reach the level of noise at 05:24:38 UTC.

Similarly, Fig. 9 shows the difference between the *PPK*(*i*) solution for height and the vertical reference daily (24 h) static solution for height, *delta H* [*PPK*(*i*) – *STATIC*]. The maximum departure from the reference daily static solution of 13 mm was registered at 05:24:15 UTC, a value that is below the level of noise (*H* showed noise within ± 24 mm). Therefore, we concluded that the heights determined by the PPK method were not significantly affected by the earthquake, *i.e.* the effects of the earthquake shaking cannot be reliably resolved from the present noise. The noise could be a result of the GNSS antenna swinging during the mainshock shake. The swinging directly influences the Easting and Northing coordinates but it also indirectly reflects on the height because the sensor is on top of a fixed pole, *i.e.* the height is not an entirely independent component causing thus a higher level of noise.

Table 3 shows obtained values of the statistical parameters, namely *Average*, *Min*, *Max*, *Range*, standard deviation (*STDEV*), and root mean square error

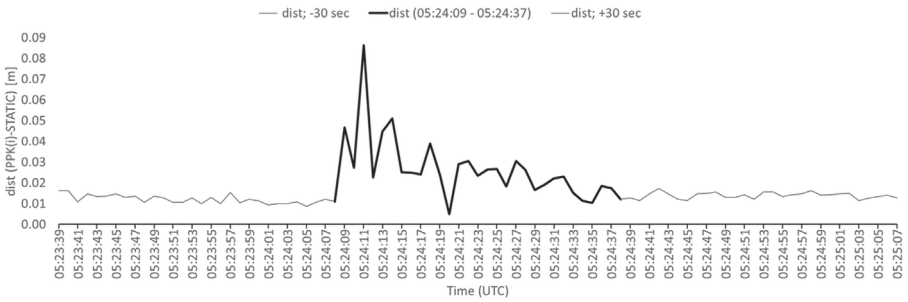

Figure 8. Distance between the *PPK(i)* solutions and the reference daily (24 h) static solution for the time segment encompassing 30 s before the earthquake-induced motion (thin grey line), the earthquake-induced motion (thick black line), and 30 s after the earthquake-induced motion attenuated into the noise (grey line). The figure shows 88 s of the signal.

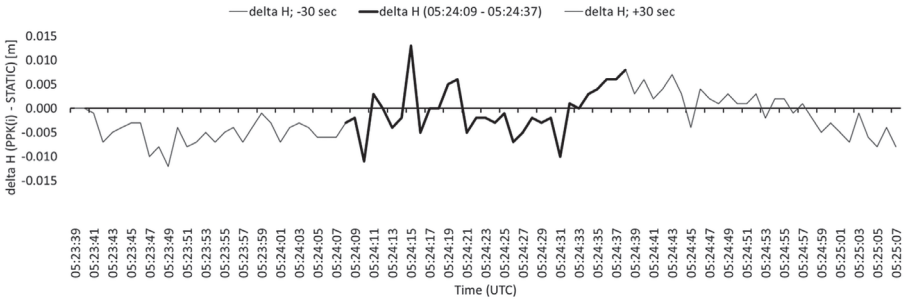

Figure 9. The height difference between each *PPK(i)* solution and the reference daily (24 h) static solution for the time window featuring the mainshock induced motion (thick black line) with an additional 30 s before its onset and after its subsidence into noise (grey lines). The figure shows 88 s of results.

(*RMSE*), for the segment of 30 s before the mainshock (–30 s), the mainshock itself (05:24:09 – 05:24:37 UTC), and the segment of 30 s after the mainshock (+30 s).

Analysing the values in Tab. 3 for horizontal component *dist* [*PPK*(*i*) – *STATIC*], it is notable that *Average*, *Range*, *STDEV* and *RMSE* are significantly larger for the mainshock shaking segment compared to the segments before (–30 s) and after (+30 s). The statistical parameters calculated for the before and after segments do not show a significant difference, therefore leading to the conclusion that they are mainly free of mainshock effects. It is worth mentioning that the quantity of relative displacement *dist* [*PPK*(*i*) – *STATIC*] is calculated according to Eq. (1), thus showing always a positive sign.

The quantity ΔH (*PPK*(*i*) – *STATIC*) shows a variable sign. Standard deviation (*STDEV*) and root mean square errors (*RMSE*) values for all three segments

Table 3. Values of statistical parameters for three segments of analysed time windows: 30 s before the mainshock, the mainshock shaking, and 30 s after the mainshock shaking.

Time window		–30 s	05:24:09–05:24:37 UTC	+30 s
dist [*PPK*(*i*) – *STATIC*] [m]	*Average*	0.012	0.027	0.014
	Max	0.016	0.086	0.017
	Min	0.009	0.005	0.011
	Range	0.008	0.081	0.006
	STDEV	0.002	0.015	0.002
	RMSE	0.012	0.031	0.014
ΔH [(*PPK*(*i*) – *STATIC*)] [m]	*Average*	–0.005	–0.001	0.000
	Max	0.000	0.013	0.008
	Min	–0.012	–0.011	–0.008
	Range	0.012	0.024	0.016
	STDEV	0.003	0.005	0.004
	RMSE	0.006	0.005	0.004

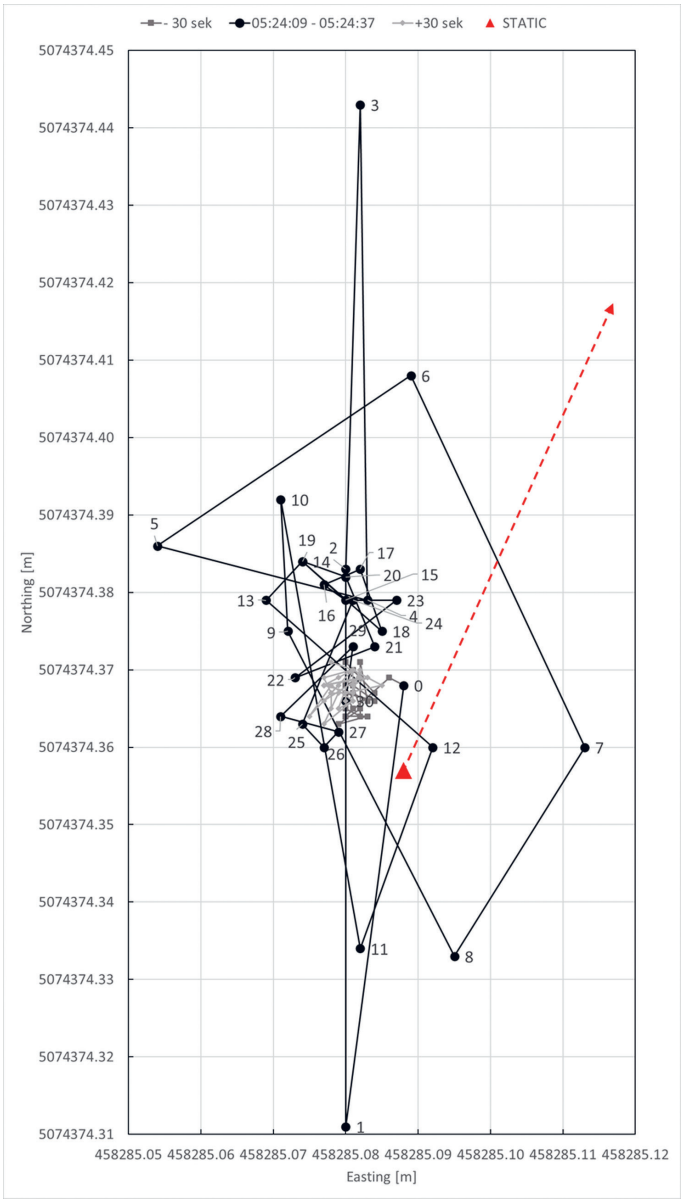

Figure 10. Kinematic effects of the $M_L = 5.5$ earthquake on the CROPOS ZAGR station derived from the PPK results on 22nd March 2020 (05:24 UTC). Black dots describe the solution for the station ZAGR during the passage of seismic waves: the numbers next to them denote the time [s] since the shaking began (the time 05:24:08 UTC is assigned as 0). Dark grey dots depict solutions in the preceding 30-seconds-long segment ("–30 s") and light grey dots show solutions for the following 30-seconds-long segment ("+30 s") after the seismic waves passed. The red triangle presents the static position (24 h) of the ZAGR station and the dashed arrow points to the earthquake epicentre (azimuth 25°).

do not show any significant differences. Anyway, *STDEV* value calculated for the mainshock shaking segment is a little bit higher (0.005 m) compared to the before (0.003 m) and after (0.004 m) segments as a consequence of the higher *Range* value of 0.024 m. Although the noise is generally present in the values for height (see Fig. 7), from Fig. 9 and Tab. 3 we can conclude that the mainshock is burdened with some bias that can be attributed to the earthquake effect.

To visualise more clearly the AGG building's motion, more specifically the motion of the GNSS antenna, caused by the passage of the seismic waves and its kinematics, the time window spanning 88 s is displayed jointly for Easting and Northing in Fig. 10.

In Fig. 10, the dark grey dots belong to the time window 30 s before the earthquake shake: they are tightly grouped, and they present the level of noise. Chronologically numbered points (solutions) display the 29-seconds-long segment of the mainshock shaking. Dot marked with the number 0 presents the solution obtained for the time 05:24:08 UTC, the next one at 05:24:09 UTC is assigned with the number 1, whereas the number 30 denotes the solution for the 05:24:38 UTC epoch. The visible effect of the earthquake starts with a polarised type of motion and the southward movement at point 1, followed by the motion to the north at point 2 and again to the south at point 3 when it turns to the west at point 4, followed by a circular type of motion: to the north-east (point 5), to the south-east (point 6), to the south-west etc. After 13 s (the dot number 13), the movement amplitude decreased to about a half of the peak value and the solutions were approaching the group of points marked with the light grey dots that present the solutions for the segment of 30 s after the earthquake shaking. Interestingly, the citizens of Zagreb often reported the shaking of 10–13 s. The maximum range in Northing of 13.2 cm occurred between points 1 and 3 along the longitudinal axis of the building (azimuth approx. 5°), whereas the maximum range in Easting of 5.9 cm was obtained between points 5 and 7. The longest distance between two consecutive PPK solutions is 7.2 cm, between points 1 and 2. The average departure of the before and after segments from the daily static solution (the dark and light grey dots), estimated as free of mainshock shaking, is 1.3 cm which can be interpreted as the bias of the PPK solutions.

3.3. Seismological consideration of the GNSS measurements

Figure 11 shows a comparison of the displacement recorded by the ZAGR GNSS station mounted on the top of the six-story (approx. 30 m high) building with the ground motion displacement simulated for the Zagreb mainshock as described in Latečki et al. (2021) at grid point closest to the Zagreb GNSS station (≈ 253 m to the north-east, azimuth ≈ 31°), for two horizontal components: E–W and N–S. In order to compare two signals, presented signals were detrended: the linear trend was removed from the simulated ground displacement components and the GNSS signal, and the GNSS signals were also demeaned. The comparison can only be qualitative and one should keep in mind that (i) the compared

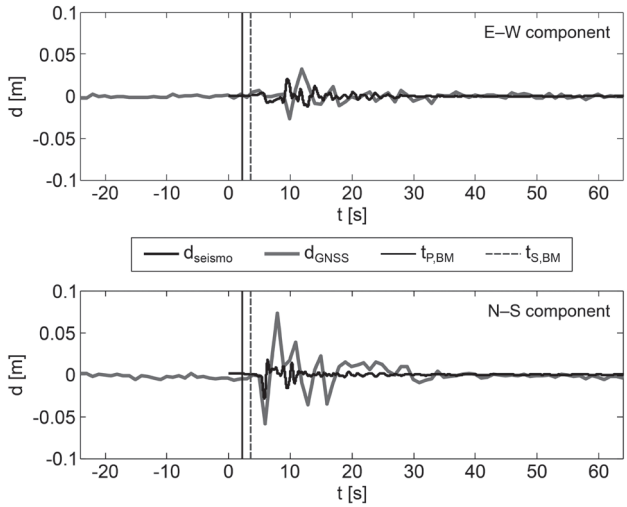

Figure 11. Comparison of the E–W and N–S component of displacement: thick black line marks simulated ground displacement for a grid point 253 m to the north-east of the ZAGR station (according to Latečki et al., 2021), while thick grey line represents the change in displacement of the ZAGR station on the top of the AGG building. The presented GNSS signal was demeaned and linearly detrended, while the simulated ground displacement signal was linearly detrended. Time t = 0 s represents earthquake origin time, while $t_{P,BM}$ and $t_{S,BM}$ present theoretical onset times for P- and S-waves according to the Balkan model.

signals do not present the same point in space, (ii) the CROPOS ZAGR station presents the response of the building to the seismic waves and not ground motion, and (iii) simulated displacement seismogram is not true ground motion recorded by a seismograph but a modelled finite-fault full-waveform simulation which is as good as the models used and methods applied. However, the figure shows some similarities. The maximum ground motion displacement was firstly achieved at the N–S component (0.029 m), whereas the maximum ground displacement on the E–W component came 3.8 s later (0.021 m). A very similar situation is seen on the recorded GNSS signal: the time elapsed between maxima of N–S and E–W components is 4 s, which is in very good agreement with the simulated ground motion displacement, and as expected, amplitudes are larger than for simulated ground motion displacement. N–S components display larger amplitudes than E–W components on both signals, especially on the GNSS displacement. Simple, basic analysis of the radiation pattern for the displacement of the point-source double couple equivalent forces (Aki and Richards, 2002), according to earthquake parameters in Tab. 2 and fault plane solution (φ = 67°, δ = 47°, λ = 79°) in Herak et al. (2021), show that the P-wave and horizontally polarized S-wave (SH-wave) should have had very small amplitude, whereas vertically polarized S-wave (SV-wave) should have displayed large amplitude. This is in good agreement with the observed and simulated displacement signals: SV-waves are polarized in the radial direction that has an azimuth of approx.

25° so the majority of the SV-waves should have been recorded on the N–S component, whereas SH-waves are in the transverse direction and they should have been recorded mostly on the E–W component. This means that the large signal on the N-S component, recorded at 5.9 s after earthquake origin time, represents S-waves whereas the large amplitudes waves that arrived later (t = 9.9 s) at the E–W component are most likely horizontally polarized surface Love waves. Larger amplitudes seen later on the N–S component are most likely Rayleigh waves with elliptical oscillations in radial and vertical plane.

Figure 12 shows a closer look at the first 10 s of the compared signals and onset times of P- and S-waves picked for the GNSS signal and the simulated ground motion together with theoretical onset times calculated according to the Balkan model (B.C.I.S., 1972). The average S-wave velocity was calculated as a ratio between hypocentral distance (12.5 km; earthquake depth is 8.3 km as in Tab. 2, the epicentral distance is 9.3 km) and the S-wave onset time. The velocity is estimated to be approx. 2.1 km/s when calculated for the onset time of the maximum amplitude at N-S component and approx. 2.6 km/s when the onset of S-wave is set to a previous measuring point (–1 s). Although the Balkan model (B.C.I.S., 1972) often used in earthquake location, sets S-waves velocity to v_S = 3.48 km/s for the homogeneous upper crust (down to 30 km of depth), the

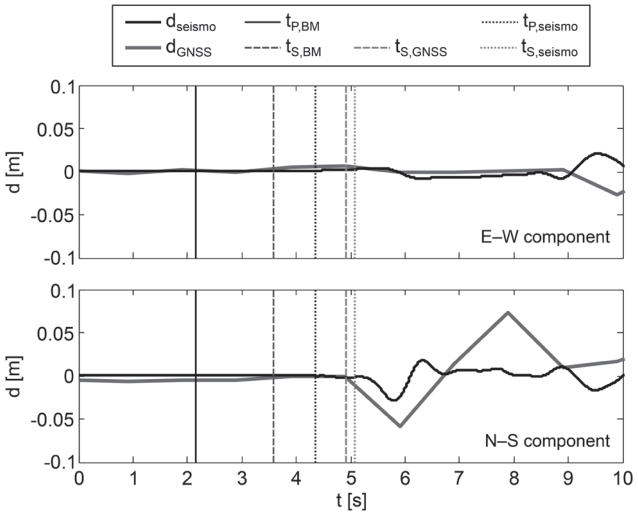

Figure 12. The first 10 s since the mainshock origin time of the simulated ground motion displacement for a grid point 253 m to the north-east of the ZAGR station (thick black line; according to Latečki et al., 2021) and change in displacement of the ZAGR station on the top of the AGG building (thick grey line). Time t = 0 s represents earthquake origin time, while $t_{P,BM}$ (thin black line) and $t_{S,BM}$ (black broken line) present theoretical onset times for P- and S-waves according to the Balkan model. The onset of the S-wave on the GNSS signal $t_{S,GNSS}$ is presented with the broken dark grey line. Dotted lines show the onset of the P- ($t_{P,seismo}$, black) and S-wave ($t_{S,seismo}$, light grey) on the simulated ground motion displacement.

Zagreb area is characterized by relatively thick and loose sediments with small velocities. Latečki et al. (2021) report for their velocity model, based on existing geological and geophysical measurements, v_S = 0.430–2.197 km/s for the sediments and v_S = 1.943–3.595 km/s for the upper crust. These low velocities in the sediments explain the low S-wave velocity calculated from the GNSS signal.

The vertical component is not considered here because of the poor vertical resolution of the GNSS measurements. Furthermore, the onset of the P-wave was hard to discriminate due to small amplitudes mostly because: (i) P-waves, in general, have several times smaller amplitudes than S-waves, (ii) the magnitude of the analysed earthquake did not generate large enough P-waves that could be recorded by the ZAGR station above the noise level, whereas (iii) fault plane geometry and relative position of the ZAGR station location to the earthquake's hypocentre location suggest that P-wave should have had very small amplitudes.

Similar results have been presented in Grapenthin and Freymueller (2011) where dynamic ground motion due to S-waves (body waves), Love waves and Rayleigh waves (surface waves) were identified from the kinematic GPS data recorded during the 2011 Tohoku-Oki earthquake, Japan.

From the seismological aspect, sampling frequency of 1 Hz is rather small compared to commonly used broadband seismographs with sampling frequency nowadays set to at least 50 Hz and accelerometers to at least 100 Hz. Therefore, it is highly possible that the ZAGR station did not record precise S-wave onset or the real maximum amplitude due to the low sampling rate. Furthermore, this low sampling rate is the most suitable for recording the surface waves. It should be taken into consideration that the motion of the building depends on the dynamic properties of the building and its response to the seismic ground motion. The building is excited into motion and is "left" to oscillate – this motion may last longer than the actual ground motion. It would be very interesting to model the response of the AGG building to the simulated ground motion and compare it with the recorded GNSS signal.

The analysis has shown that the GNSS station measurements and the PPK method applied to it can record and reproduce S- and surface waves of a close moderately strong earthquake. Furthermore, these can be used for approximate estimation of the S-wave onset for a strong enough and close enough earthquake.

4. Conclusions

The motion of the CROPOS ZAGR station mounted on the top of the AGG building in the Zagreb city centre during the Zagreb 2020 M_L = 5.5 earthquake was analysed by the Post-Processed Kinematic (PPK) method in reference to the ZABO station at a distance of about 25 km to the north. All available GNSS signals were used: GPS, GLONASS, Galileo and BeiDou. In order to kinematically assess earthquake effects, permanent GNSS observations logged at a rate of 1 Hz were analysed. This is the first time that a significant earthquake with

the epicentre in Croatia was kinematically examined and seismologically interpreted using data from GNSS stations of the CROPOS network.

Only the mainshock (22nd March 2020 05:24 UTC), with an epicentre located about 9 km to the north-northeast from the ZAGR station, was detected in the PPK results even though four aftershocks with $M_L \geq 2.5$ occurred in the 5–6 UTC time window. The movements caused by mainshock shaking were in the range of 13.2 cm for Northing and 5.9 cm for Easting. The range of 4.7 cm for the height component of the PPK solutions corresponding to the fluctuations of ± 24 mm around the static daily solution was estimated as statistically not significant because it is just above the level of noise. Although the kinematic behaviour of the ZAGR station was notable during the shake, permanent displacement was not identified. The analysis showed that the PPK method has the potential to detect the effects of moderately strong earthquake shaking as well as to assess a kinematic behaviour of a GNSS station even at relatively large distances (*e.g.* 25 km). The ability to use Galileo and BeiDou systems within the CROPOS network improved the possibility to assess the earthquake effect on the GNSS antenna directly and indirectly on the structure it is mounted on.

The qualitative comparison of the ZAGR station displacement induced by earthquake shaking and the displacement simulated for the Zagreb earthquake scenario for the closest grid point are in a reasonable agreement. Furthermore, seismological consideration showed that S-waves and surface waves were detected by the GNSS sensor: S-waves were recorded on the N–S component as vertically polarized S-waves (SV-waves) while Love waves dominate in the E-W component. However, the sampling frequency of 1 Hz is too low for most seismological purposes, *e.g.* the determination of the precise onset times and earthquake location. A permanent GNSS network with smaller distances between stations and higher observation frequency (*e.g.* 10 Hz) could be beneficial for the assessment of earthquake effects.

Acknowledgements – The authors kindly acknowledge the Croatian Seismological Survey of the Department of Geophysics, Faculty of Science, University of Zagreb and its head Mrs Ines Ivančić, M. Sc. for providing data about $M_L \geq 2.5$ earthquakes registered on 22nd March 2020 in the epicentral area of Medvednica mountain. USGS and EMSC are acknowledged for providing data about earthquakes. Additionally, we acknowledge the State Geodetic Administration (SGA) of the Republic of Croatia for providing GNSS observation data collected at stations of the CROPOS network. We thank Helena Latečki for providing us with the data of the Zagreb $M_L = 5.5$ ground motion simulations and additional information used in the seismological consideration.

References

Aki, K. and Richards, P.G. (2002): *Quantitative seismology*. 2nd Edition. Sausalito, University Science Books.

Bačić, Ž., Šugar, D. and Grzunov, R. (2017): Investigation of GNSS Receiver's Accuracy Integrated on UAVs, *FIG Working Week 2017 Surveying the world of tomorrow – From digitalisation to augmented reality*, FIG – International Federation of Surveyors, May 29–June 2, 2017, Helsinki, Finland.

B.C.I.S. (1972): Tables des temp de propagation des ondes séismiques (Hodochrones) pour la region des Balkans, Manuel d'utilisation, Bureau Central International de Séismologie, Strasbourg.

Benedicto, J. and Da Costa, R. (2020): Directions 2021: Galileo expands and modernizes global PNT, GPS World, **31**(12), 27–29 and 34, https://www.gpsworld.com/directions-2021-galileo-expands-and-modernizes-global-pnt/ (last accessed on July 3rd, 2021).

Blaženka, D., Bačić, Ž. and Šugar, D. (2018): Ispitivanje navigacijske točnosti besposadnih letjelica, 5. CROPOS konferencija – Zbornik radova, (edit.) Marjanović, M., Pavasović, M., Zagreb: Državna geodetska uprava (DGU), Sveučilište u Zagrebu – Geodetski fakultet (GEOF), Hrvatsko geodetsko društvo (HGD), Hrvatska komora ovlaštenih inženjera geodezije (HKOIG), 43–53 (in Croatian).

Blecha, J. (2018): Trimble Business Center: Modernized Approaches for GNSS Baseline Processing, Trimble Inc. Westminster, Colorado, USA, https://geospatial.trimble.com/sites/geospatial.trimble.com/files/inline-files/TBC_Modernized%20Approaches%20for%20GNSS%20Baseline%20Processing_WHP_USL_0818.pdf (last accessed July 3rd, 2021).

Dasović, I., Herak, D., Herka, M., Latečki, H., Mustać, M., Tomljenović, B. (2020): O potresima u Hrvatskoj, *Vijesti Hrvatskoga geološkog društva*, 57/1, godina XLVII, 4–27, Zagreb (in Croatian).

Estey, L. and Wier, S. (2014): *Teqc tutorial: Basics of Teqc use and Teqc products*. UNAVCO, Boulder, Colorado, USA.

European GNSS Agency (2020): GNSS User Technology Report, **3**, https://www.gsa.europa.eu/sites/default/files/uploads/technology_report_2020.pdf.

European-Mediterranean Seismological Centre (2020): M 5.4 – CROATIA – 2020-03-22 05:24:02 UTC, https://www.emsc-csem.org/Earthquake/earthquake.php?id=840695#summary, (accessed July 3rd, 2021).

European Space Agency (2021a): ESA signs contract for new generation of Galileo, https://www.esa.int/Applications/Navigation/ESA_signs_contract_for_new_generation_of_Galileo, (last accessed on July 3rd, 2021).

European Space Agency (2021b): Two new satellites mark further enlargement of Galileo, https://www.esa.int/Applications/Navigation/Two_new_satellites_mark_further_enlargement_of_Galileo, (last accessed on December 15th, 2021).

Ganas, A., Elias, P., Briole, P., Cannavo, F., Valkaniotis, S., Tsironi, V. and Partheniou, E. I. (2020): Ground Deformation and Seismic Fault Model of the M6.4 Durres (Albania) Nov. 26, 2019 Earthquake, Based on GNSS/INSAR Observations, *Geosciences*, **10**, 210, https://doi.org/10.3390/geosciences10060210.

Glaner, M. and Weber, R. (2021): PPP with integer ambiguity resolution for GPS and Galileo using satellite products from different analysis centers, GPS Solut 25, 102, https://doi.org/10.1007/s10291-021-01140-z.

Govorčin, M. (2020): https://twitter.com/govorcin/status/1242433684168413186 (last accessed on July 3rd, 2021).

Grapenthin, R. and Freymueller, J. T. (2011): The dynamics of a seismic wave field: Animation and analysis of kinematic GPS data recorded during the 2011 Tohoku-Oki earthquake, Japan, Geophys. Res. Lett., **38**, L18308, https://doi.org/10.1029/2011GL048405.

Herak, M., Herak, D. and Orlić, N. (2021): Properties of the Zagreb 22 March 2020 earthquake sequence – analyses of the full year of aftershock recording, *Geofizika*, **38**, 93–116, https://doi.org/10.15233/gfz/2021.38.6.

Herak, M., Allegretti, I., Herak, D., Ivančić, I., Kuk, V., Marić, K., Markušić, S. and Sović, I. (2011): Republika Hrvatska. Karta potresnih područja, Sveučilište u Zagrebu – Prirodoslovno-matematički fakultet, Geofizički odsjek, available online at http://seizkarta.gfz.hr/ (in Croatian).

Hofmann-Wellenhof, B., Lichtenegger, H. and Wasle, E. (2008): *GNSS – Global Navigation Satellite Systems – GPS, GLONASS, Galileo, and more*. Springer-Verlag Wien, New York, https://doi.org/10.1007/978-3-211-73017-1.

Hohensinn, R. and Geiger, A. (2018): Stand-alone GNSS sensors as velocity seismometers: Real-time monitoring and earthquake detection, *Sensors*, **18**, 3712, https://doi.org/10.3390/s18113712.

Ivančić, I., Herak, D., Herak, M., Allegretti, I., Fiket, T., Kuk, K., Markušić, S., Prevolnik, S., Sović, I., Dasović, I. and Stipčević, J. (2018): Seismicity of Croatia in the period 2006 – 2015, *Geofizika*, **35**, 69–98, https://doi.org/10.15233/gfz.2018.35.2.

Kliman, A. (2021): *Satelitski sustav Galileo i njegova implementacija kroz modernizaciju CROPOS-a*. Diploma Thesis, University of Zagreb – Faculty of Geodesy, Zagreb, Croatia (in Croatian).

Kouba, J., Lahaye, F., and Tétreault, P. (2017): Precise point positioning, in: *Springer Handbook of Global Navigation Satellite Systems*, edited by Teunissen, P. J. G. and Montenbruck, O. 723–751.

Larson, K. M., Bodin, P. and Gomberg, J. (2003): Using 1-Hz GPS data to measure deformations caused by the Denali fault earthquake, *Science*, **300**, 1421–1424, https://doi.org/10.1126/science.1084531.

Latečki, H., Molinari, I. and Stipčević, J. (2021): Seismic shaking scenarios for city of Zagreb, Capital of Croatia, *Bull. Earthq. Eng.*, https://doi.org/10.1007/s10518-021-01227-5.

Li, X., Ge, M., Guo, B., Wickert, J. and Schuh, H. (2013): Temporal point positioning approach for real-time GNSS seismology using a single receiver, *Geophys. Res. Lett.*, **40**, 5677–5682, https://doi.org/10.1002/2013GL057818.

Lipatnikov, L. A. and Shevchuk, S. O. (2019): *Cost effective precise positioning with GNSS*. FIG Commission 5, The International Federation of Surveyors (FIG), Copenhagen, Denmark.

Magaš, K. (2021): Utjecaj modernizacije CROPOS-a na service sustava. Diploma Thesis, Faculty of Geodesy, University of Zagreb, Zagreb, Croatia (in Croatian).

Markušić, S., Stanko, D., Korbar, T., Belić, N., Penava, D. and Kordić, B. (2020): The Zagreb (Croatia) M5.5 earthquake on 22 March 2020, *Geosciences*, **10**, 252, https://doi.org/10.3390/geosciences10070252.

Maufroid, X., Pont, G. and Benedicto, J. (2021): Galileo Status. *Munich Satellite Navigation Summit*, Munich, 16–17th March 2021.

Paziewski, J., Kurpinski, G., Wielgosz, P., Stolecki, L., Sieradzki, R., Seta, M., Oszczak, S., Castillo, M. and Martin-Porqueras, F. (2020): Towards Galileo + GPS seismology: Validation of high-rate GNSS-based system for seismic events characterisation, *Measurement*, **166**, 108236, https://doi.org/10.1016/j.measurement.2020.108236.

Rizos, C., Janssen, V., Roberts, C. and Grinter, T. (2012): Precise point positioning: Is the era of differential GNSS positioning drawing to an end?, *FIG Working Week 2012*, Rome, Italy.

Seismological Survey, Department of Geophysics, Faculty of Science, University of Zagreb (2020): Pola godine od Zagrebačkog potresa, http://www.pmf.unizg.hr/geof/seizmoloska_sluzba/o_zagrebackom_potresu_2020/pola_godine_od_potresa# (last accessed on April 29th, 2021) (in Croatian).

Šavor Novak, M., Uroš, M., Atalić, J., Herak, M., Demšić, M., Baniček, M., Lazarević, D., Bijelić, N., Crnogorac, M. and Todorić, M. (2020): Zagreb earthquake of 22 March 2020 – Preliminary report on seismologic aspects and damage to buildings, *Građevinar*, **72**, 843–867, https://doi.org/10.14256/JCE.2966.2020.

Šugar, D. and Bačić, Ž. (2021): Kinematic effects of M5.5 Zagreb earthquake assessed by GNSS method supported by Galileo satellite system, in: *Proceedings of the 1st Croatian Conference on Earthquake Engineering – 1CroCEE*, edited by Lakušić, S. and Atalić, J., Faculty of Civil Engineering, University of Zagreb, Zagreb, Croatia, 385–395, https://doi.org/10.5592/CO/1CroCEE.2021.

Šugar, D., Sučić, P. and Bačić, Ž. (2016): Examination of site suitability for GNSS measurements, SIG2016 – in: *Proceedings of the International Symposium on Engineering Geodesy*, edited by: Paar, R., Marendić, A. and Zrinjski, M., Croatian Geodetic Society, Varaždin, Croatia, 255–266.

Šugar, D., Skopljak, B. and Bačić, Ž. (2018): Multi-constellation GNSS baseline solutions – A perspective from the user›s and developer›s point of view, FIG – 2018 Congress Proceedings – Embracing our smart world where the continents connect: enhancing the geospatial maturity of societies, FIG – International Federation of Surveyors, May 6–11, 2018, Istanbul, Turkey.

TEQC, https://www.unavco.org/software/data-processing/teqc/teqc.html (last accessed on July 3rd, 2021).

Tomljenović, B. (2020): Osvrt na potres u Zagrebu 2020. godine, https://www.rgn.unizg.hr/hr/izdvojeno/2587-osvrt-na-potres-u-zagrebu-2020-godine-autor-teksta-je-prof-dr-sc-bruno-tomljenovic, (last accessed on July 3rd, 2021).

United States Geological Survey (2020): M 5.3 – 5 km E of Gornja Bistra, Croatia, https://earthquake.usgs.gov/earthquakes/eventpage/us70008dx7/executive (last accessed on July 3rd, 2021).

Weston, N. D. and Schwieger, V. (2014): *Cost effective GNSS positioning techniques*. FIG Commission 5 Publication, 2nd Edition, The International Federation of Surveyors (FIG), Copenhagen, Denmark.

Xu, P., Shi, C., Fang, R., Liu, J., Niu, X., Zhang, Q. and Yanagidani, T. (2013): High-rate precise point positioning (PPP) to measure seismic wave motions: An experimental comparison of GPS PPP with inertial measurement units, *J. Geod.*, *87*, 361–372, https://doi.org/10.1007/s00190-012-0606-z.

Zumberge, J. F., Heflin, M. B., Jefferson, D. C., Watkins, M. M. and Webb, F. H. (1997): Precise point positioning for the efficient and robust analysis of GPS data from large networks, *J. Geophys. Res.*, **102(B3)**, 5005–5017, https://doi.org/10.1029/96JB03860.

SAŽETAK

Geodetska i seizmološka analiza kinematike CROPOS ZAGR stanice tijekom zagrebačkog potresa M_L 5,5 2020. godine

Danijel Šugar, Željko Bačić i Iva Dasović

CROPOS-ova (*Croatian Positioning System*) stanica ZAGR jedna je od 33 stanice hrvatske permanentne mreže GNSS (*Global Navigation Satellite System*), a nalazi se u središtu grada Zagreba na krovu zgrade u kojoj su smještena tri fakulteta Sveučilišta u Zagrebu (Geodetski, Građevinski i Arhitektonski fakultet). Po prvi puta su analizirani učinci potresa na jednu od stanica mreže CROPOS primjenom metode PPK (*Post-Processed Kinematic*) koristeći signale svih dostupnih globalnih navigacijskih satelitskih sustava: GPS, GLONASS, Galileo i BeiDou – i to efekti zagrebačkog potresa M_L = 5,5 iz 2020. godine na stanicu ZAGR udaljenu približno 9 km od epicentra potresa. Analiza je pokazala da su pomaci stanice ZAGR, kao kombinirana gibanja površine i zgrade, tijekom potresne trešnje bili daleko iznad razine šuma što je omogućilo procjenu kinematičkog ponašanja stanice: gibanja su bila u smjeru sjever-jug u rasponu približno 13 cm i približno 6 cm u rasponu u smjeru istok-zapad. Gibanja u vertikalnom smjeru identificirana su tek neznatno iznad razine šuma. Iako je kinematičko gibanje stanice ZAGR bilo izraženo i jasno vidljivo, nije utvđen nikakav permanentan pomak kao posljedica potresa. Seizmološka analiza pokazala je da je stanica ZAGR zabilježila početak SV-valova na komponenti sjever-jug, površinske Rayleigheve valove na komponenti sjever-jug te površinske Loveove valove na komponenti istok-zapad. Jednosekundni (1 Hz) rezultati omogućili su detaljnu analizu kinematičkog ponašanja stanice ZAGR kao što su i ukazali na korisnost metode PPK za određivanje učinaka potresa.

Ključne riječi: CROPOS, GNSS, kinematičko gibanje, potres, PPK metoda

Corresponding author's address: Danijel Šugar, Faculty of Geodesy, University of Zagreb, Kačićeva 26, HR-10000 Zagreb, Croatia; e-mail: dsugar@geof.hr; ORCID: https://orcid.org/0000-0002-7796-9915